NON PARAMETRIC DISTORTION CORRECTION IN ENDOSCOPIC MEDICAL IMAGES

Joao P. Barreto[1], *Rahul Swaminathan*[2], *and Jose Roquette*[1]

Institute for Systems and Robotics[1]
Dept. of Electrical and Computer Engineering
University of Coimbra, Portugal

Deutsche Telekom Labs[2]
and Technische Universität Berlin
Berlin, Germany

ABSTRACT

Endoscopes consisting of a probe mounted with a camera head, are frequently used in medicine for inspection and visualization of human body cavities (knee and shoulder articulations, bronchi, nose, brain, etc). However the images often suffer from strong lens distortions. Estimation and correction of image distortion is important not only to improve the practitioner's perception of the inspected area but also to develop systems for 3D navigation and computer assisted surgery.

In this paper we compare various conventional calibration methods against the new parameter free method proposed by Hartley and Kang. We believe the non-parametric method is more suitable for endoscopic imaging. We present numerical analysis of the goodness of fit of other conventional approaches as well as calibration results on real images. It should be noted that our results are directly applicable to all vision applications using wide-angle lenses.

***Index Terms*—** Calibration, lens distortion, radial distortions, non-perspective, endoscope.

1. INTRODUCTION

Endoscopic imaging is increasingly becoming standard practice as minimally invasive surgery gains acceptance. This is a relatively simple approach to imaging the interior of the body for both surgical as well as preventive care. The acquired image is typically directly relayed to the surgeons for visualization. However, the images suffer from strong lens distortions. Physical constraints on the size of the probe, the tubular structure as well as the need to visualize a large field of view necessitate the use of wide-angle lenses leading to lens distortions [1] as seen in Fig.1.

Lens distortions, affect the spatial perception of the interiors visualized by the users. While humans are accustomed to "seeing" the world around perspectively, these distorted images do not adhere to the laws of perspective projection. Moreover, any geometric analysis of the imagery such as building $3D$ models, or computing the pose of the probe relies on first estimating (calibrating for) the lens distortion. This means that the relation between pixels in the image and projective rays in the 3D space must be estimated.

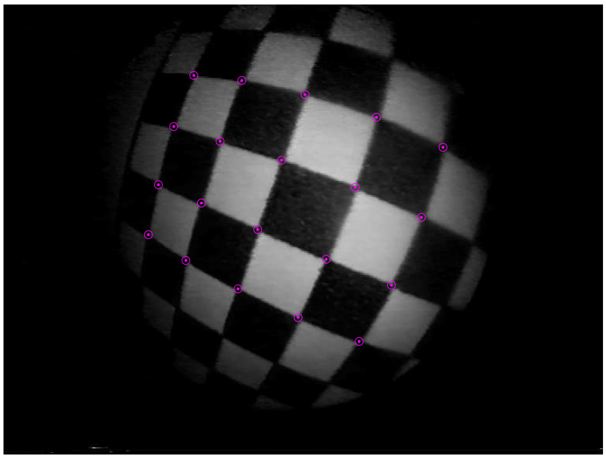

Fig. 1. Endoscopic image exhibiting strong non-linear lens distortions. User selects grid points (red) for calibration.

The calibration of perspective cameras is a well studied subject (see [2]). Similarly many approaches have been developed for wide-angle lens distortion correction (see [3, 4, 5, 6, 7]). These methods typically rely on choosing a distortion model whose parameters are then estimated. In endoscopes and arthroscopes, such a distortion model choice is not always obvious. We therefore propose to use a non-parametric method proposed by Hartley and Sing-Bing Kang [8].

In this paper we present initial results of applying the non-parametric calibration [8] to endoscopic images. We also present a comparison with conventional calibration methods such as Bouguet [9] and the division model [10]. Furthermore, we show how conventional radial distortion models fail to fit distortion profiles of the endoscopic images. We finally present a comparison of methods applied to real images.

2. METHOD

We use a planar pattern with points on a known grid for distortion calibration. Also we assume the lens to have only radial distortions, about an unknown center of distortion. We use a non-parametric approach [8], initially proposed by Hartley and Kang, to estimate the center of distortion $\mathbf{e}$ as well as the radial distortion across the image. Since the approach is non-parametric, for every point $\mathbf{x_i^d}$ along the radial direction we compute the undistorting "scale" factor λ_i, given by: $\mathbf{x_i^d} = \mathbf{e} + \lambda_i.(\mathbf{x_i^u} - \mathbf{e})$.

2.1. Computing the Distortion Center

Hartley and Kang used the relationship between the grid points and the distorted image points, as two views of an unknown scene under camera motion. Thus, the planar pattern itself is considered as one view, while the distorted image is another view. Distortions typically pull the image points towards a distortion center. This is similar to the camera moving away from the scene. Thus, the image epipole actually corresponds to the center of distortion.

We use $N = 43$ images of the calibration grid. In every image the user selects M_i ($1 \leq i \leq N$) points $\mathbf{x^d}$ that correspond to the known grid points $\mathbf{x_c}$. For every image we then compute the fundamental matrix $\mathbf{F_i}$ as well as the image epipole (distortion center) e_i ($(\mathbf{x_i^d})^T \mathbf{F_i} \mathbf{x_i^c} = 0$). Since all the images share the same distortion center, we can estimate a single effective distortion center $\mathbf{e}$ using all the fundamental matrices in a least squares sense: $[\mathbf{F_1}^T; \mathbf{F_2}^T; \ldots; \mathbf{F_N}^T] \cdot \mathbf{e} = 0$

2.2. Computing Radial Distortions

We use the distortion center computed earlier to now compute the radial distortion component. We first note that the calibration grid used is planar. Therefore, for every image i, there exists an *homography* $\mathbf{H_i}$ that maps the grid points $\mathbf{x_i^c}$ to the undistorted image points $\mathbf{x_i^u}$:

$$\mathbf{x_i^u} = \mathbf{H_i}.\mathbf{x_i^c} \tag{1}$$

We first enforce the epipole (distortion center) of every image to lie at the origin$(0, 0, 1)^T$. After transforming the image points appropriately, we recompute the fundamental matrices of the form $\hat{\mathbf{F}} = [\mathbf{f_1}^T; \mathbf{f_2}^T; \mathbf{0}]$. Then the desired homography per image is given by: $\mathbf{H_i} = [\mathbf{f_2}^T; -\mathbf{f_1}^T; \mathbf{v_i}^T]$, where $\mathbf{v_i}^T$ is unknown. The estimation of the exact radial distortion essentially reduces to estimating the correct $\mathbf{v_i}^T$ for every image. As pointed out by Hartley and Kang, this was solved in [11] assuming a parameterized distortion model. However, in the non-parametric case it can also be solved under the assumption that: (1) distortion is radial and symmetric about the center of distortion (thus assuming square pixels), and (2) that the distortion is monotonic increasing. It should be pointed out that the method is completely linear and extremely efficient. For further details we direct the reader to [8].

3. EXPERIMENTAL EVALUATION

In this section we present experimental results of applying the calibration method to images acquired with an endoscope. More importantly we present comparisons between the non-parametric approach and other conventional model based methods. Furthermore, we present results on the "goodness of fit" of various conventional models to the measured radial distortions.

3.1. Estimation of Distortion Center

The first step to estimating radial distortions is to determine the center of distortion e. Referring to the algorithm presented in section 2, we estimate the center of distortion using 43 images. Due to noise in user selected points, these estimates vary a lot as seen in Fig.2. We also show here the effective distortion center estimated using all the fundamental matrices simultaneously as well as the principal point estimate using the conventional Conrady model[12]. Note that the principal point, computed using the Bouguet calibration toolkit, [9] is very close to the effective distortion center. The slight variation can be attributed to noise.

3.2. Estimating Radial Distortions.

Using the Hartley-Kang method we can compute the radial distortion present at every user clicked image grid point (blue point cloud in Fig.1). Thus, in some sense we "measure" directly the radial distortion at points at various distances from the distortion center. We now compare results obtained using the parameter free approach and model based conventional methods.

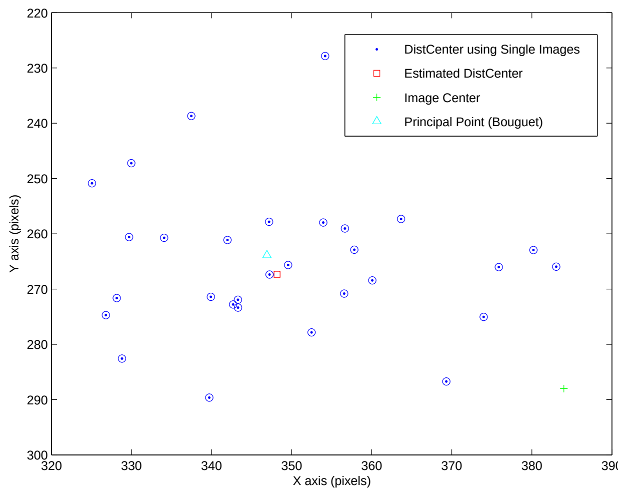

Fig. 2. Plot showing the variance in the estimated center of distortion across the set of acquired images. The centers are individually estimated by decomposing the individual fundamental matrices as described in Section2. Also shown are the effective distortion center computed using all the F matrices simultaneously and the principal point estimated using Bouguet[9].

In Fig. 3 (a,b) we show a plot of the distorted radial distances against the estimated undistorted distances across the image (blue dots). We first test the goodness of fit of conventional radial distortion models (see Tab.1[12, 3]) to the estimated radial distortion profile computed using the non-parametric approach. As seen in Fig 3(a), the conventional models (see Tab.1 for details) do not fit the data well.

In Fig 3(b), we compare standard calibration techniques to the non-parametric approach. Again it is clear from the plots that both these methods do not perform well with this imaging sensor. While Bouguet, under fits the distortion, the division model performs over estimation. In contrast, a simple 1 parameter quadratic model provides a much better fit. This suggests that the polynomial model used for radial distortions greatly influences calibration.

To better visualize the deficiency of conventional calibration methods we now compare the undistorted images. We begin by first comparing the results using the Hartley-Kang method (non-parametric undistortion using the estimated homographies $\mathbf{H_i}$) against the Bouguet toolkit. Fig. 4 shows a region of the imaged grid points and their undistorted positions using both approaches. As seen, Bouguet underestimates the distortion which is visible by the fact that the "undistorted" points do not lie on a straight line. In contrast, the non-parametric approach estimates the distortion more accurately.

Method	Model
Radial 3^{rd} Order	$r_d = r_u + \xi_1 r_u^3$
Radial 5^{th} Order	$r_d = r_u + \xi_1 r_u^3 + \xi_2 r_u^5$
Bouguet (Conrady [12])	$r_d = r_u + \xi_1 r_u^3 + \xi_2 r_u^5$
Radial 2^{nd} Order	$r_d = r_u + \xi_1 r_u^2$
Division Model	$r_u = \frac{r_d}{1+\xi_1 r_d^2}$

Table 1. Models used for the distortion curve fitting.

Finally the real image (Fig. 1) is undistorted as shown in Fig. 5 using (a) Bouguet calibration, (b) the division model and (c) the Hartley-Kang non-parametric method (using the polynomial fitting). While Bouguet(a) under-estimates the distortions, the division model seems to over-estimate them. Surprisingly, the quadratic model fitted to the distortion profile computed using the Hartley-Kang approach does a much better at distortion modeling.

4. CONCLUSION

We compared traditional distortion calibration methods (Bouguet and division model) against a non-parametric approach [8]. We found that these conventional methods failed to estimate distortions in endoscopic images robustly. We therefore performed goodness of fit tests using conventional polynomial models for the radial distortion component. Surprisingly, these models did not fit the distortion profile of endoscopic images.

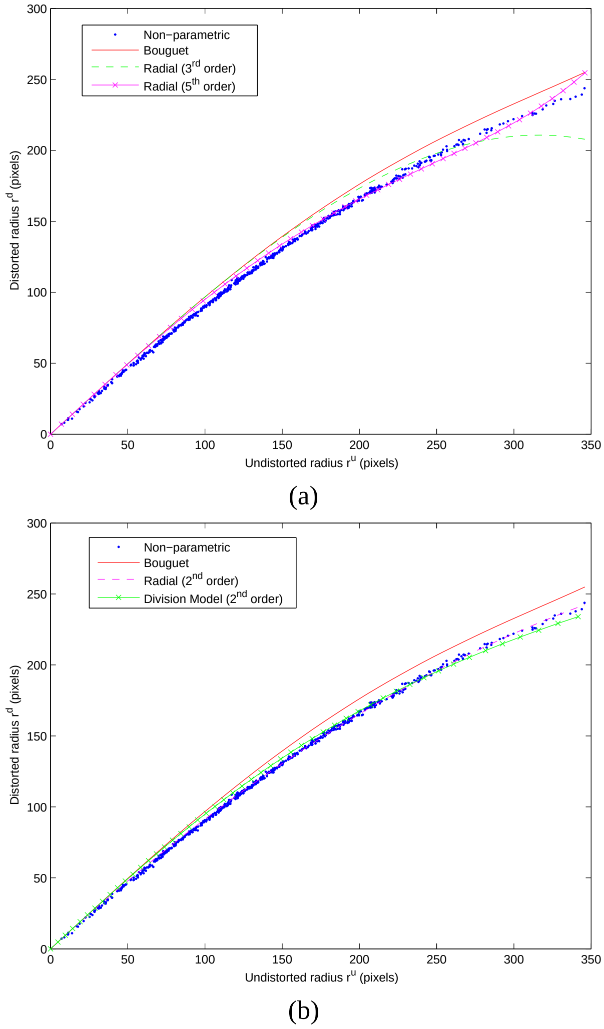

Fig. 3. Fitting of various distortion models to the estimated distortion curve. In (a) we fit the standard $3^r d$ order, and 5^{th} order radial distortion models to the distortion profile. In (b) we compare between the radial model used in the Bouguet toolbox, the division model and a simple quadratic model. From these plots it is clear that conventional models do not fir the radial distortion profile well.

Hence we recommend a two step approach to lens distortion calibration consisting of first performing non-parametric distortion estimation and followed by "appropriate" model fitting. Although we address endoscopic imaging, our results are directly applicable to any vision application using wide-angle lenses.

ACKNOWLEDGMENTS

The authors are grateful to "Fundacao da Ciencia e Tecnologia" for support through the grant POSC/SRI/45970/2002–CAMIDES. They would also like to thank Fernando Fonseca, MD and "Hospitais da Universidade de Coimbra" for allowing us to collect the endoscopic images.

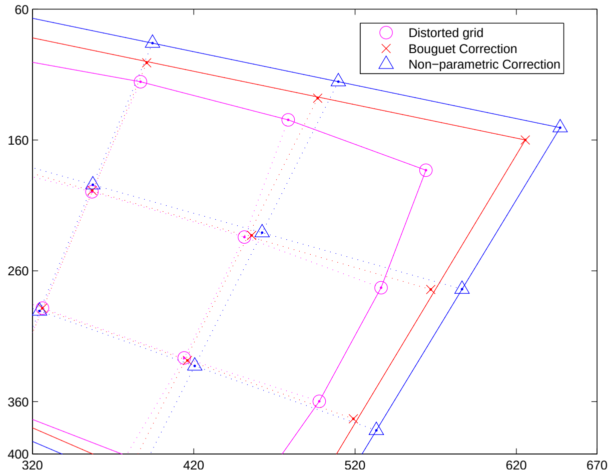

Fig. 4. Undistortion performed to user selected points in the acquired image using Bouguet calibration (using radial distortions) as well as the non-parametric approach. Bouguet underestimates the distortions and consequently the points do not lie on a straight line. In contrast the non-parametric approach performs better.

5. REFERENCES

[1] M. Born and E. Wolf, *Principles of Optics*, Permagon Press, 1965.

[2] R. Hartley, "Estimation of relative camera positions for uncalibrated cameras," in *ECCV*, 1992, pp. 579–587.

[3] D.C. Brown, "Close range camera calibration," *Photogrammetric Engineering*, vol. 37, no. 8, pp. 855–866, 1971.

[4] S. B. Kang, "Semi-automatic methods for recovering radial distortion parameters from a single image," *DEC, Cambridge Research Labs, Technical Reports Series CRL 97/3*, 1997.

[5] G.P. Stein, "Lens distortion calibration using point correspondences," in *Proc. CVPR*, 1997, pp. 143–148.

[6] R. Swaminathan and S.K. Nayar, "Nonmetric calibration of wide-angle lenses and polycameras," *PAMI*, vol. 22, no. 10, pp. 1172–1178, 2000.

[7] J. P. Barreto and K. Daniilidis, "Fundamental-Matrix for Cameras with Radial Distortion," in *ICCV*, 2005.

[8] R. I. Hartley and S. B Kang, "Parameter-Free Radial Distortion Correction with Centre of Distortion Estimation," in *ICCV*, 2005, pp. II: 1834–1841.

[9] Z Zhang, "Flexible Camera Calibration by Viewing a Plane from Unknown Orientations," in *ICCV*, 1999, pp. 666–673.

[10] C. Brauer-Burchardt and K. Voss, "A new algorithm to correct fish-eye- and strong wide-angle- lens-distortion from single images," in *ICIP*, 2001.

[11] S. Thirthala and M. Pollefeys, "The Radial Trifocal Tensor: A Tool for Calibrating the Radial Distortion of Wide-Angle Cameras," in *CVPR*, 2005, pp. I: 321–328.

[12] A. Conrady, "Decentering lens systems," *Monthly notices of the Royal Astronomical Society*, vol. 79, pp. 384–390, 1919.

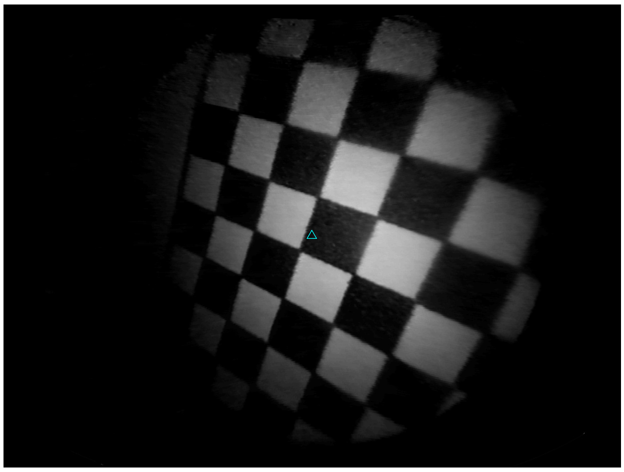

(a)

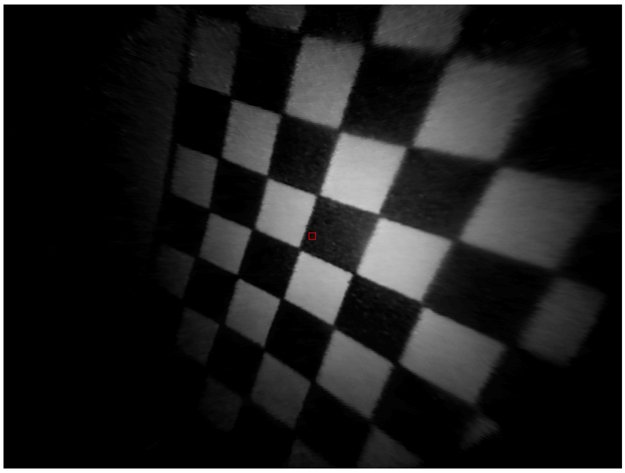

(b)

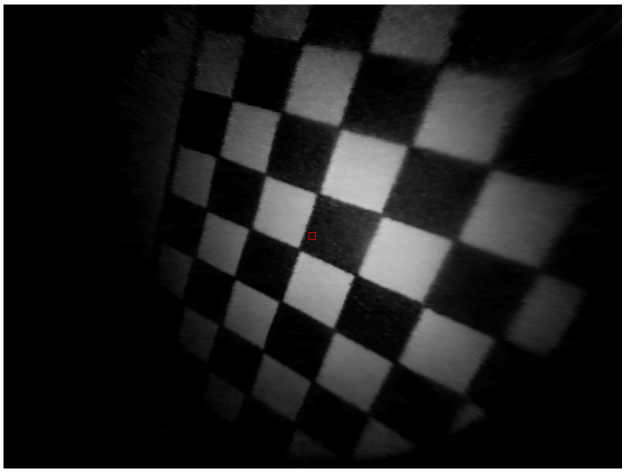

(c)

Fig. 5. Results of image undistortion using (a) Bouguet–clearly, (b) the division model and (c) quadratic model fitted to the distortion profile. Surprisingly the unconventional quadratic model fitted to estimates from the Hartley-Kang method outperforms traditional methods.